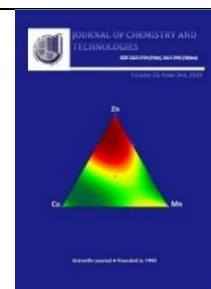




Journal of Chemistry and Technologies

pISSN 2663-2934 (Print), ISSN 2663-2942 (Online)

journal homepage: <http://chemistry.dnu.dp.ua>



UDC 549.731.11: 544.478-03

SYNTHESIS, STRUCTURAL, MAGNETIC AND PHOTOCATALYTIC PROPERTIES OF MFe_2O_4 ($M = Co, Mn, Zn$) FERRITE NANOPARTICLES OBTAINED BY PLASMACHEMICAL METHOD

Liliya A. Frolova, Tatyana V. Hrydnieva

Ukrainian State University of Chemical Technology, Dnipro, Ukraine

Received 2 September 2020; accepted 16 October 2020; available online 4 November 2020

Abstract

Composite ferrites MFe_2O_4 ($M = Co, Mn, Zn$) were synthesized by plasma method. X-ray phase analysis, vibration magnetometry spectroscopic analysis, simplex-lattice planning of the experiment were used to characterize the obtained samples. The photocatalytic activity of the compounds was studied in the decomposition reaction of 4-nitrophenol, which was used as a model organic contaminant. It was found that the obtained ferrite nanoparticles have a spinel structure. The change in the lattice parameter occurs depending on the radius of the substitution cation and the location of the ions on the sublattices. The minimum values of the lattice parameter and the maximum saturation magnetization and coercive force correspond to the double compositions of Mn-Co ferrites. The synthesized nanoferrites have a band gap between 1.55 and 1.9 eV. All $Zn_{1-x}Co_xFe_2O_4$ ferrites and $Zn_{1-x}Co_xMn_{0.5}Fe_2O_4$ ($0 < x < 1$) were found to have high catalytic activity.

Key words: synthesis, ferrites, photocatalysts, magnetic characteristics

СИНТЕЗ, СТРУКТУРНІ, МАГНІТНІ ТА ФОТОКАТАЛИТИЧНІ ВЛАСТИВОСТІ ФЕРИТОВИХ НАНОЧАСТИНОК MFe_2O_4 ($M = Co, Mn, Zn$), ОТРИМАНИХ ПЛАЗМОХІМІЧНИМ МЕТОДОМ

Лілія А. Фролова, Тетяна В. Гриднєва

ДВНЗ «Український державний хіміко-технологічний університет», Дніпро, Україна

Анотація

Плазмовим методом синтезовані композиційні ферити $MeFe_2O_4$ ($Me = Co, Mn, Zn$). Для характеристики отриманих зразків було використано рентгенофазовий аналіз, вібраційну магнітometriю спектроскопічний аналіз, симплекс-решітчасте планування експерименту. Фотокаталітичну активність сполук вивчали в реакції розкладання 4-нітрофенолу, який використовували як модельний органічний забруднювач. Встановлено, що отримані наночастинки феритів мають шпінельну структуру. Зміна параметру решітки відбувається в залежності від радіуса катіона замішувача та розташування іонів по підрешіткам. Мінімальні значення параметру решітки та максимальні намагніченість насичення та коерцитивна сила відповідають подвійним складам Mn-Co феритів. Синтезовані наноферити мають енергію забороненої зони між 1.55 і 1.9 eV. Встановлено, що всі $Zn_{1-x}Co_xFe_2O_4$ ферити та $Zn_{1-x}Co_xMn_{0.5}Fe_2O_4$ ($0 < x < 1$) мають високу каталітичну активність.

Ключові слова: синтез, ферити, фотокаталіз, магнітні характеристики

*Corresponding author: tel.: +380973846557; e-mail: 19kozak83@gmail.com

© 2020 Oles Honchar Dnipro National University

doi: 10.15421/082022

СИНТЕЗ, СТРУКТУРНЫЕ, МАГНИТНЫЕ И ФОТОКАТАЛИТИЧЕСКИЕ СВОЙСТВА ФЕРРИТНЫХ НАНОЧАСТИЦ MFe_2O_4 ($M = Co, Mn, Zn$), ПОЛУЧЕННЫХ ПЛАЗМОХИМИЧЕСКИМ МЕТОДОМ

Лилия А. Фролова, Татьяна В. Гриднева

ГВУЗ «Украинский государственный химико-технологический университет», Днепро, Украина

Аннотация

Плазменным методом синтезированы композиционные ферриты $MeFe_2O_4$ ($Me = Co, Mn, Zn$). Для характеристики полученных образцов были использованы рентгенофазовый анализ, вибрационная магнитометрия, спектроскопический анализ, симплекс-решетчатое планирование эксперимента. Фотокаталитическую активность соединений изучали на реакции разложения 4-нитрофенола, который использовали как модельный органический загрязнитель. Установлено, что полученные наночастицы ферритов имеют шпинельной структуру. Изменение параметра решетки происходит в зависимости от радиуса катиона заместителя и расположения ионов по подрешеткам. Минимальные значения параметра решетки и максимальные намагниченность насыщения и коэрцитивная сила соответствуют двойным составам Mn-Co-ферритов. Синтезированные наноферриты имеют энергию запрещенной зоны между 1.55 и 1.9 эВ. Установлено, что все $Zn_{1-x}Co_xFe_2O_4$ ферриты и $Zn_{1-x}Co_xMn_{0.5}Fe_2O_4$ ($0 < x < 1$) имеют высокую каталитическую активность.

Ключевые слова: синтез, ферриты, фотокатализ, магнитные характеристики

Introduction

Spinel structures have been widely used in various industries for many years [1–3]. A special place is occupied by nanodispersed spinel ferrites MFe_2O_4 (where M is an ion of a divalent transition metal), for example, Ni, Co, Cu, Mn, Zn are very interesting magnetic materials and attract the attention of researchers due to their unique magnetic, electrical, catalytic, and optical properties [4–6].

The use of ferrites in ecological technologies for the decomposition of organic compounds is promising [7–10]. Researchers have been searching for a simple, fast and economical method for the degradation of various phenolic compounds in aqueous solutions for many years. Numerous oxidation and reduction methods for the removal of organic compounds are known, such as photocatalytic degradation, electrochemical processes, hydrogenation reactions, etc. [10–12]. A very common method of removing 4-NP from industrial wastewater by reducing it to 4-aminophenol (4-AP) [13–15]. Very promising are photocatalytic processes of decomposition of 4-nitrophenol in the presence of catalysts.

Ferrites, being an important class of magnetic materials, are also used as catalysts for the degradation of 4-NP [16–18]. The choice of ferrites as catalysts is very promising due to the simplicity and economic feasibility of the synthesis process, their resistance to strongly acidic and alkaline reaction medium. High magnetic properties make it easy to separate them from the reaction mixture.

In [18–20], the possibility of using magnetic nanoparticles $CoFe_2O_4$, $ZnFe_2O_4$, $NiFe_2O_4$, $CuFe_2O_4$ for decomposition and reduction of organic compounds was studied. The comparative catalytic efficiency of XFe_2O_4 ($X = Mn, Fe, Ni, Co$, and Zn) nanoferrites [21] showed that $NiFe_2O_4$ is the best catalyst among all non-doped ferrites. At present, technologies for the production of dispersed spinel ferrites, such as ceramic, mechanical activation, solvothermal, sonochemical, sol-gel, coprecipitation, have been developed [22–26]. But the above methods for the synthesis of ferrites require synthesis at high temperature or pressure, the use of organic reagents. In addition, classical technologies are multi-stage and are often accompanied by inefficient and cumbersome stages of raw material preparation and do not allow to obtain complex single-phase ferrites at low temperatures [24]. The method of coprecipitation allows to realize such advantages as high product activity, high specific surface area, cheap raw materials, low energy consumption, unique physical and chemical properties compared to consolidated structures [25]. Previous microscopic studies have shown the possibility of obtaining nanodispersed ferrites by plasma treatment of coprecipitated hydroxides [26–28].

The aim of this work is the synthesis of ferrites of the general formula MFe_2O_4 ($M = Co, Mn, Zn$) and the study of their structural, magnetic and catalytic properties in the decomposition reaction of 4-nitrophenol by simplex the lattice method of experimental design. To compare the catalytic efficiency and determine the effect of cations on

the properties, ten samples of ferrites were synthesized and studied in detail.

Experimental part

For the synthesis of samples (Table 1) iron(II) sulfate, cobalt sulfate, manganese sulfate, zinc sulfate, sodium hydroxide of analytical purity were used.

Ferrites with the general formula $MeFe_2O_4$ (Me = Co, Mn Zn,) were synthesized using the plasma method, which is described in more detail in [26; 29]. Radiographs of the samples were obtained on the device DRON-2.0 under monochromatic $CoK\alpha$ radiation. The size of the crystallites was determined using the Debye-Scherrer formula.

Determination of magnetic characteristics was performed using a vibrating magnetometer. EPR spectra were obtained using a Radiopan SE/X-2543 radio spectrometer. Signal intensity and resonant frequency were used to characterize the EPR signals.

UV-VS spectroscopy was used to analyze the optical properties of powdered ferrites. The results were used to calculate the energy of the band gap. The band gap energy was determined from the diffuse reflection spectra of the samples using the Kubelka-Munch function.

Studies of the catalytic decomposition of 4-NP were performed in a glass vessel at 25 °C with constant shaking. As a radiation source was used UV lamp DKB 9 with an effective spectral range of 180-275 nm. The intensity of ultraviolet radiation was about 3 mW/cm². The lamp was placed above the solution at a distance of 10 cm from its surface. Before adding the catalyst, the maximum absorption of the model solution was measured using a UV 5800 PC spectrophotometer. in the range of 200–900 nm.

The degree of decomposition was calculated by the formula:

$$\%X = \frac{(C_0 - C_t) \cdot 100\%}{C_0} \quad (1)$$

where: C_0 is the initial concentration of 4-NP in solution, mol/l,

C_t is the concentration of 4-NP in the solution at time t, mol/l.

To study the effect of the cationic composition on the properties of ferrites, a simplex lattice plan was used, which requires a minimum number of experiments to study the influence of factors on the selected reaction functions. The molar concentrations of cobalt, manganese and zinc, respectively, were chosen as factors x_1, x_2, x_3 . The plan of the experiment is shown in table 1.

Table 1

Planning matrix of the simplex - lattice method {3,3}

Nº sample	Formula	Co	Mn	Zn	y
1	$CoFe_2O_4$	1.00	0	0	y_1
2	$Co_{0.67}Mn_{0.33}Fe_2O_4$	0.667	0.33	0	y_{122}
3	$Co_{0.33}Mn_{0.67}Fe_2O_4$	0.333	0.667	0	y_{112}
4	$MnFe_2O_4$	0	1.00	0	y_2
5	$Mn_{0.67}Zn_{0.33}Fe_2O_4$	0	0.667	0.33	y_{223}
6	$Mn_{0.33}Zn_{0.67}Fe_2O_4$	0	0.333	0.667	y_{233}
7	$ZnFe_2O_4$	0	0	1.00	y_3
8	$Co_{0.33}Zn_{0.67}Fe_2O_4$	0.33	0	0.667	y_{133}
9	$Co_{0.67}Zn_{0.33}Fe_2O_4$	0.667	0	0.333	y_{113}
10	$Co_{0.33}Zn_{0.33}Mn_{0.33}Fe_2O_4$	0.333	0.333	0.333	y_{123}

Diagrams of the «properties of the composition» were constructed using isolines. The response functions were coercion (Hc), Oe; saturation magnetization (M_s), Emu/g; a is the lattice parameter, Å; X_{4NP} - degree of decomposition of 4-NP, %, E - gap band energy, eV.

Results and discussions

Characteristics of ferrite samples. Fig. 1 shows the radiographs of the powder samples corresponding to table 2. The radiographs have indexed peaks (111), (220), (311), (222), (400), (422), (511) and (440), as shown in the figure 1. Indexed peaks correspond to the typical spinel phase. There is a decrease in the intensity and

expansion of the peak with increasing manganese concentration in the ferrites $Mn_xCo_{1-x}Fe_2O_4$ and $Mn_xZn_{1-x}Fe_2O_4$ ($0 < x < 1$) (samples 1-4, 4-7). The most intense peaks correspond to cobalt-zinc ferrites. With increasing zinc content, the degree of crystallinity of ferrites increases.

Weak diffuse scattering at a small angle indicates the presence in the studied materials along with the crystalline phases of a small amount of substance in the X-ray amorphous state. X-ray diffraction patterns also show broad peaks, indicating the nanodispersed nature and small crystal size of the samples.

The lattice parameter increases with increasing zinc concentration in $Zn_xCo_{1-x}Fe_2O_4$

formulations. The minimum values correspond to double compositions at $x > 0.55$. A more pronounced increase in the lattice parameter is observed for samples 1-4, a small 4-7 and a

decrease of 8-10. This indicates the replacement of the smaller Co^{2+} ion (0.72 Å) by the larger Mn^{2+} ion (0.80 Å) and, accordingly, Mn^{2+} (0.80 Å) by Zn^{2+} (0.74 Å) (Fig. 2, Table 2).

Table 2

The results of the experiments

N	Co	Mn	Zn	H_c , Oe	M_s , Emu/g	H_R , mT	I_R , a. u.	a, Å	E, eV	X_{4NP} , %
1	1	0	0	1124	105,41	547	2662	8,3516	1,58	87,75
2	0,667	0,333	0	706	69,16	501	3237	8,341	1,72	89,82
3	0,333	0,667	0	370	73,05	444	1000	8,3573	1,82	68,11
4	0	1	0	41	111,79	352	2322	8,3592	1,55	88,58
5	0	0,667	0,333	8	47,7	307	2851	8,3430	1,71	71,08
6	0	0,333	0,667	8	3,75	343	2439	8,366	1,82	88,9
7	0	0	1	19	3,93	342	3044	8,3689	1,9	83,49
8	0,333	0	0,667	1	3,26	382	2537	8,3795	1,75	90,35
9	0,667	0	0,333	70	74,94	501	1137	8,3487	1,63	83,45
10	0,3333	0,3333	0,3333	0	9,72	350	3123	8,36025	1,59	82,26

In complex zinc manganese ferrites, the replacement of a smaller zinc ion by a larger Mn^{2+} cation in manganese-zinc ferrite causes a decrease in the constant lattice. This anomalous behavior can be explained by the fact that manganese ferrite is a mixed spinel and a significant proportion of Mn^{2+} and Zn^{2+} occupy octahedral positions and convert Fe^{3+} cations into tetrahedral

regions against their chemical advantages. Since Fe^{3+} ions have a smaller ionic radius (0.64 Å), their replacement in tetrahedral positions by the content of larger divalent ions leads to a decrease in the lattice parameter. This fact may also explain the change in the magnetic properties of manganese-zinc ferrites.

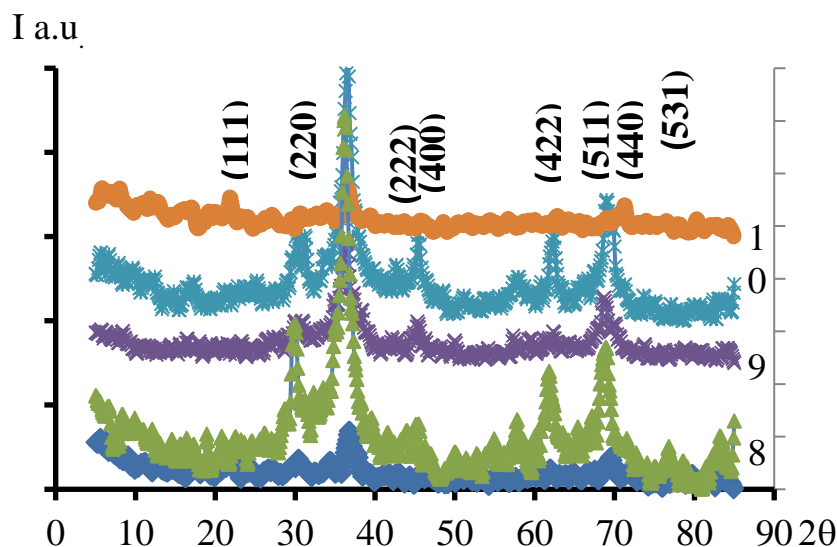
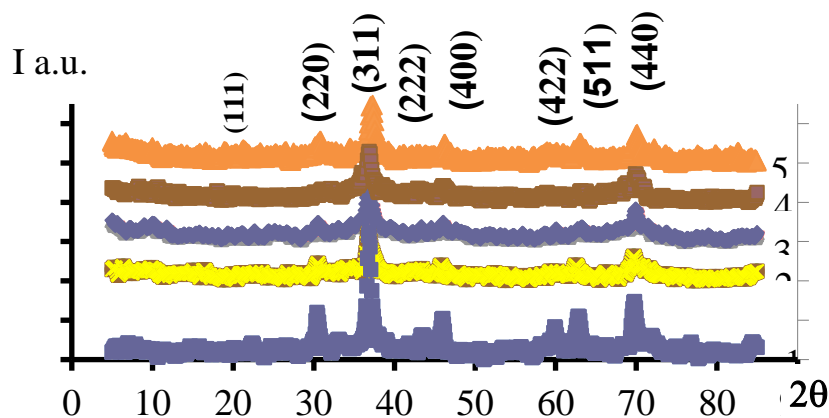


Fig. 1 X-ray patterns of ferrites: a – samples 1, 2, 3, 4, b – samples 6,7,8,9,10

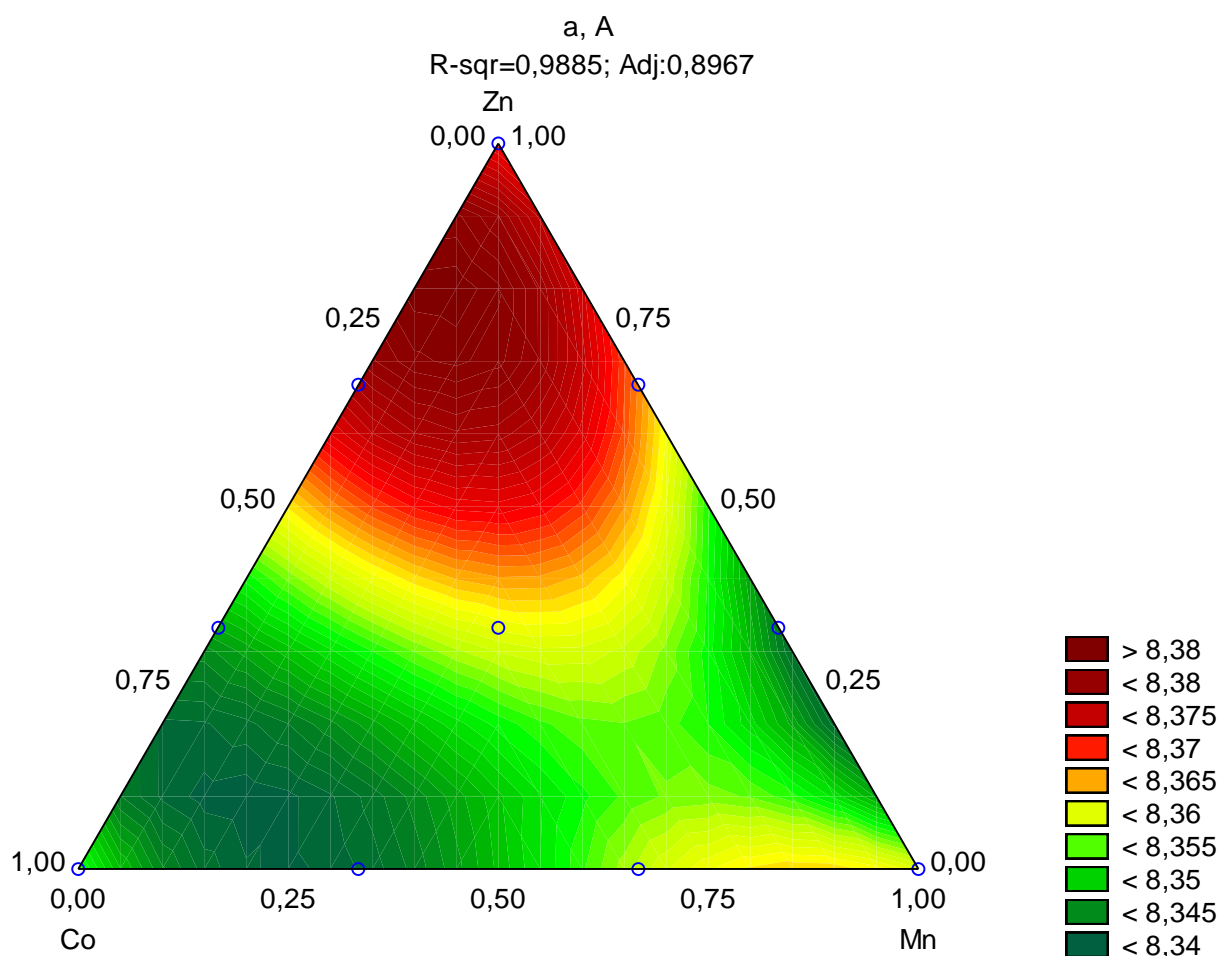


Fig. 2 Dependence of the lattice parameter on the composition of ferrites

Magnetic properties. The saturation magnetization (Ms) and the coercive force (Hc) derived from the magnetization curves are shown in Fig.3. The magnetic characteristics of the material are the most important properties, which are determined by recording values (8.32 Å), as well as by increasing the bandwidth on magnetization curves at room temperature. Increasing the cobalt content in the system leads to an increase in the coercive force and saturation magnetization. The increase in the coercive force and saturation magnetization correspond to MnFe_2O_4 and CoFe_2O_4 (Ms is 111.8 Emu/g and 105.41 Emu/g, respectively).

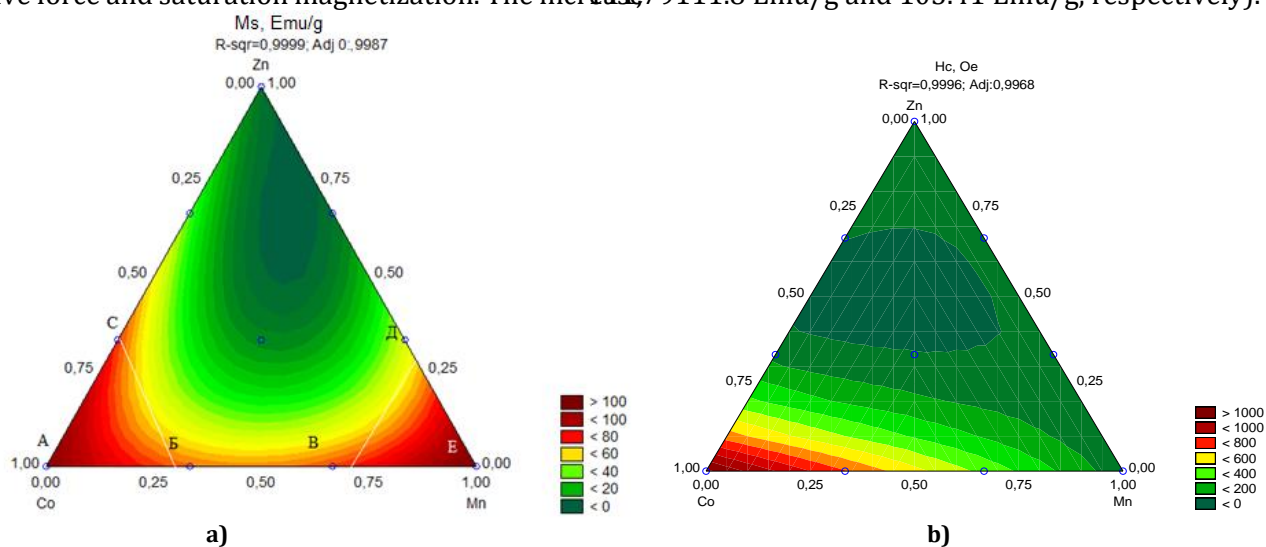


Fig. 3 Dependence of magnetic characteristics on the composition of ferrites: a – saturation magnetization, b – coercive force

Moreover, the value of the saturation magnetization depends to a greater extent on the content of cobalt cations. The highest magnetic values correspond to the maximum cobalt content. Thus, magnetic ferrites with high coercive force correspond to compositions 1, 2, 3, and magnetic ferrites with low coercive force to compositions 4, 5, 6, 7. The diagrams can be divided into two equilateral triangles with coordinates of the vertices A (0, 1, 0) - B (0.25, 0.75, 0) - C (0, 0.75, 0.25) and B (0,0,1) E (0.25, 0.75, 0) D (0, 0.75, 0.25) which corresponds to the region of higher values of saturation magnetization.

Optical characteristics. Diffuse reflection spectra were obtained to evaluate the optical properties of ferrites. All 10 samples showed an intense absorption band in the UV region of the electromagnetic spectrum. The width of the band

gap in the samples was determined by the equation

$$\alpha h\nu = A (h\nu - E)^n, n = 2$$

where α is the absorption coefficient, ν is the frequency of light, E is the energy of the band gap, eV, and A is the proportionality constant.

The band gap calculated for CoFe_2O_4 , MnFe_2O_4 , ZnFe_2O_4 was 1.58 eV, 1.59 eV, 2.2 eV, respectively, and were slightly lower than those reported in [23; 24].

The energy of the ferrite band gap is shown in Table 2. It increases with increasing Zn content (Fig. 2a). A significant change in the values of the energy of the band gap can be observed due to the difference in the average size of the crystallites, constant lattice, phase purity, the concentration of the charge carrier and the deformation of the crystal lattice.

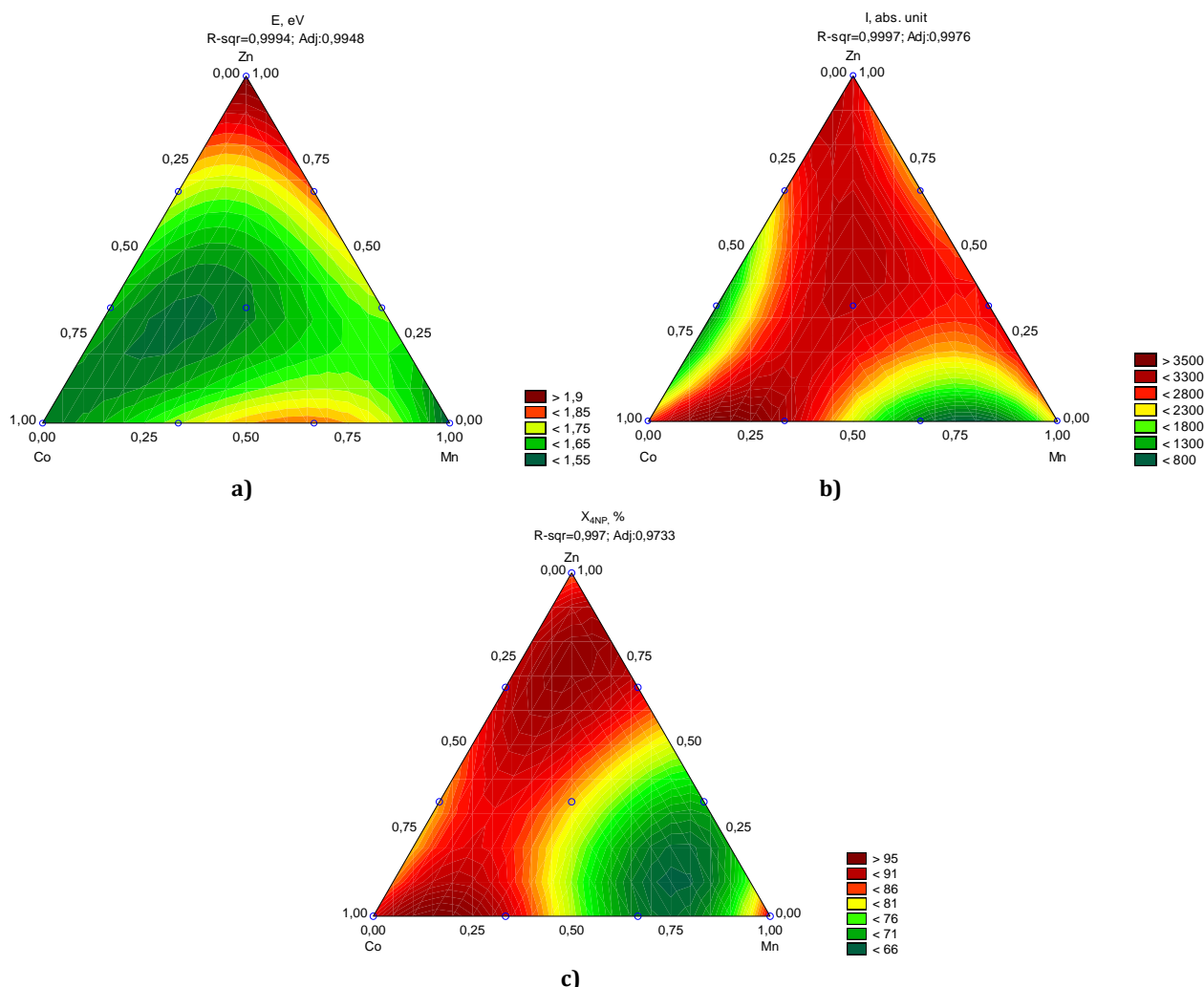


Figure 4. Dependence of the energy of the band gap on the composition (a), the peak intensity on the EPR spectrum (b), the degree of decomposition of 4-NP on the composition (c)

Comparison of diagrams of the dependences of the energy of the band gap on the composition and intensity of the EPR peak of the spectrum makes it

possible to determine which of the above factors is the most influential (Fig. 4).

The results of processing the spectra of electronic paramagnetic resonance (EPR) of

photocatalysts are shown in Fig.4b. Two indicators of the intensity of the EPR peak of the spectrum and the value of the resonant frequency were chosen as an evaluation criterion. Zn^{2+} ions with a more filled d orbital do not contribute to the EPR signal of the spectrum in the case of an excited state. The dependence of the peak intensity on the number of electrons in the last orbital can be clearly seen. For a cobalt atom, the number d of electrons is 7, zinc 10, manganese 5.

Photocatalytic properties. Studies of the photocatalytic activity of ferrites showed that the degree of decomposition of 4-NP in the presence of ferrite photocatalysts was 70–90 % for 60 min under UV radiation. The decomposition kinetics of 4-NP in the presence of ferrites are presented in

Experiments have shown that 4-NP cannot undergo spontaneous decomposition without UV irradiation, both in the presence and in the absence of a catalyst. The destruction of 4-NP molecules occurs in solutions that are exposed only to UV radiation, this process is significantly accelerated in the presence of ferrite catalysts.

From Fig. 4c shows that the photocatalytic activity is highest for cobalt zinc ferrites and cobalt zinc manganese ferrites, while the manganese content should not exceed 0.55. The results of the reactivity of individual ferrites, much lower than the double and triple compositions (Table 2).

Conclusions

For use as photocatalysts, ferrites MFe_2O_4 ($M = Co, Mn, Zn$) were synthesized by a combined method of coprecipitation and subsequent plasma treatment.

The regularities of changes in the properties of ferrites are investigated by the simplex-lattice method of experimental design. The obtained ferrites were characterized by X-ray phase analysis, EPR spectroscopy, UV spectroscopy, vibration magnetometry.

Nanoparticles synthesized by coprecipitation and plasma treatment have a cubic spinel structure.

The minimum values of the lattice parameter and the maximum saturation magnetization and coercive force correspond to the double compositions of Mn-Co ferrites. The synthesized nanoferrites have a band gap of 1.55 to 1.9 eV. It was found that all ferrites $Zn_{1-x}Co_xFe_2O_4$ and $Zn_{1-x}Co_xMn_{0.5}Fe_2O_4$ ($0 < x < 1$) have high catalytic activity.

The band gaps for $CoFe_2O_4$, $MnFe_2O_4$, $ZnFe_2O_4$ were 1.58 eV, 1.55 eV, 1.9 eV, respectively. With an

increase in the Zn content, it increases from 1.63 to 1.9 eV.

The role of the cation in the decomposition of 4-NP is established. The most effective catalysts are composite ferrites containing cobalt-zinc-manganese, while the manganese content should not exceed 0.55.

Bibliography

- [1] Mastering surface reconstruction of metastable spinel oxides for better water oxidation / Y. Duan, S. Sun, Y. Sun [et al.] // *Advanced materials*. – 2019. – Vol. 31. – N 12. – P. 1807898.
- [2] Zaichuk A. V. Blue-green spinel-type ceramic pigments prepared from the slag of aluminothermal production of ferrotitanium / A.V. Zaichuk, A. A. Amelina // *Вопросы химии и химической технологии*. – 2019. – Vol. 4. – P. 46–54.
- [3] Zhao X. Two-dimensional Spinel Structured Co-based Materials for High Performance Supercapacitors: A Critical Review / X. Zhao, L. Mao, Q. Cheng, J. Li // *Chemical Engineering Journal*. – 2020. – Vol. 387. – P. 124081.
- [4] Almessiere M. A. Magneto-optical properties of rare earth metals substituted Co-Zn spinel nanoferrites / M. A. Almessiere, A. Korkmaz, Y. Slimani [et al.] // *Ceramics International*. – 2019. – Vol. 45. – N 3. – P. 3449–3458.
- [5] Structural and Magnetic Properties of Spinel Ferrite Nanoparticles / F. G. D. Silva, J. Depeyrot, A. F. C. Campos [et al.] // *Journal of nanoscience and nanotechnology*. – 2019. – Vol. 19. – N 8. – P. 4888–4902.
- [6] Structural, magnetic, optical properties and cation distribution of nanosized $Ni_{0.3}Cu_{0.3}Zn_{0.4}Tm_xFe_{2-x}O_4$ ($0.0 \leq x \leq 0.10$) spinel ferrites synthesized by ultrasound irradiation / Y. Slimani, M.A. Almessiere, M. Sertkol, S. E. Shirsath // *Ultrasonics sonochemistry*. – 2019. – Vol. 57. – P. 203–211.
- [7] Rani M. Efficient photocatalytic degradation of Bisphenol A by metal ferrites nanoparticles under sunlight / M. Rani, U. Shanker // *Environmental Technology & Innovation*. – 2020. – P. 100792.
- [8] Lassoued A. Magnetic and photocatalytic properties of Ni-Co ferrites / A. Lassoued, J. F. Li // *Solid State Sciences*. – 2020. – C. 106199.
- [9] Javed H. Reduced graphene oxide-spinel ferrite nano-hybrids as magnetically separable and recyclable visible light driven photocatalyst / H. Javed, A. Rehman, S. Mussadiq [et al.] // *Synthetic Metals*. – 2019. – Vol. 254. – P. 1–9.
- [10] Sonochemical synthesis of $NiFe_2O_4$ nanoparticles: Characterization and their photocatalytic and electrochemical applications / M.A. S. Amulya, H.P. Nagaswarupa, M.R. Anil Kumar [et al.] // *Applied Surface Science Advances*. – 2020. – Vol. 1. – P. 100023.
- [11] Fadillah G. Enhanced electrochemical degradation of 4-Nitrophenol molecules using novel Ti/TiO₂-NiO electrodes / G. Fadillah, T. A. Saleh, S. Wahyuningsih //

- Journal of Molecular Liquids. – 2019. – Vol. 289, – P. 111108.
- [12] Photoelectrocatalytic degradation of amino-azodyes by titanium dioxide with surface states of Ti^{3+} /G. V. Sokolsky, M. N. Zahornyi, T.F. Lobunets [et al.] // Journal of Chemistry and Technologies. – 2019. – Vol. 27, N 2. – P. 130–140.
- [13] Ayodhya D. Influence of g-C₃N₄ and g-C₃N₄ nanosheets supported CuS coupled system with effect of pH on the catalytic activity of 4-NP reduction using NaBH₄ / D. Ayodhya, G. Veerabhadram // Chemistry of Flat Materials. – 2019. – Vol. 14. – P. 100088.
- [14] Abdullah H. Utilization of photocatalytic hydrogen evolved (Zn, Sn)(O, S) nanoparticles to reduce 4-nitrophenol to 4-aminophenol /H. Abdullah, D.H. Kuo // International Journal of Hydrogen Energy. – 2019. – Vol. 44, N 1. – P. 191–201.
- [15] [15] Liao G. Unlocking the door to highly efficient Ag-based nanoparticles catalysts for NaBH₄-assisted nitrophenol reduction [Text] / G. Liao, Y. Gong, L. Zhong, J. Fang [et al.] // NanoResearch. – 2019. – P. 1–30.
- [16] Kharisov B. I. Mini-review: ferrite nanoparticles in the catalysis / B.I. Kharisov, H. R. Dias, O. V. Kharissova // Arabian Journal of Chemistry. – 2019. – Vol. 12, N 7. – P. 1234–1246.
- [17] Frolova L. Photocatalytic activity of spinel ferrites Co_xFe_{3-x}O₄ (0.25 < x < 1) obtained by treatment contact low-temperature non-equilibrium plasma liquors / L. Frolova // Applied Nanoscience. – 2020. – P. 1–6.
- [18] A high performance recyclable magnetic CuFe₂O₄ nanocatalyst for facile reduction of 4-nitrophenol / C. Dey, D. De, M. Nandi, M. M. Goswami // Materials Chemistry and Physics. – 2020. – Vol. 242. – P. 122237.
- [19] Ce–Nd Co-substituted nanospinel cobalt ferrites: an investigation of their structural, magnetic, optical, and apoptotic properties / M. A. Almessiere, Y. Slimani, M. Sertkol [et al.] // Ceramics International. – 2019. – Vol. 45, N 13. – P. 16147–16156.
- [20] On the reversible deactivation of cobalt ferrite spinel nanoparticles applied in selective 2-propanol oxidation / S. Anke, T. Falk, G. Bendt [et al.] // Journal of Catalysis. – 2020. – Vol. 382. – P. 57–68.
- [21] An experimental and theoretical study on the structure and photoactivity of XFe₂O₄ (X= Mn, Fe, Ni, Co, and Zn) structures / M. Padervand, M. Vossoughi, H. Yousefi [et al.] // Russian Journal of Physical Chemistry A. – 2014. – Vol. 88, N 13. – P. 2451–2461.
- [22] Anupama A. V. Synthesis of highly magnetic Mn-Zn ferrite (Mn_{0.7}Zn_{0.3}Fe₂O₄) ceramic powder and its use in smart magnetorheological fluid /A.V. Anupama, V. Kumaran, B. Sahoo // Rheologica Acta. – 2019. – Vol. 58, N 5. – P. 273–280.
- [23] Melo R. S. Hydrothermal synthesis of nickel doped cobalt ferrite nanoparticles: optical and magnetic properties /R. S. Melo, P. Banerjee, A. Franco // Journal of Materials Science: Materials in Electronics. – 2018. – Vol. 29, N 17. – P. 14657–14667.
- [24] Structural, optical and magnetic properties of Mn_xFe_{3-x}O₄ nanoferrites synthesized by a simple capping agent-free coprecipitation route / S. T. Yazdi, P. Iranmanesh, S. Saeednia, M. Mehran // Materials Science and Engineering: B. – 2019. – Vol. 245. – P. 55–62.
- [25] Frolova L. Synthesis of pigments in Fe₂O₃-Al₂O₃-CoO by co-precipitation method / L. Frolova, A. Pivovarov, T. Butyrina // Pigment & Resin Technology. – 2017. – Vol. 46, N 5. – P. 356–361.
- [26] Frolova L. Non-equilibrium plasma-assisted hydrophaseferritization in Fe²⁺-Ni²⁺-SO₄²⁻-OH- System / L. Frolova, A. Pivovarov, E. Tsepich // Nanophysics, Nanophotonics, Surface Studies, and Applications. Springer Proceedings in Physics. – 2016. –Vol. 183. – P. 213–220.
- [27] Frolova L. Ultrasound ferritization in Fe²⁺-Ni²⁺-SO₄²⁻-OH- system / L. Frolova, A. Pivovarov, E. Tsepich // Journal of Chemical Technology and Metallurgy. – 2016. – Vol. 51, N 2. – P. 163–167.
- [28] Frolova L. A. The Effect of Contact Non-equilibrium Plasma on Structural and Magnetic Properties of Mn_xFe_{3-x}O₄ / L. A. Frolova, M. P. Derhachov // Spinels. Nanoscale research letters. – 2017. – Vol. 12, N 1. – P. 505.
- [29] Frolova L. Structural and magnetic properties of cobalt ferrite nanopowders synthesis using contact non-equilibrium plasma / L. Frolova, A. Derimova, T. Butyrina // Acta Physica Polonica A. – 2018. – Vol. 133, N 4. – P. 1021–1023.

References

- [1] Duan, Y., Sun, S., Sun, Y., Xi, S., Chi, X., Zhang, Q., Ren, X., Wang, J., Du, Y., Grimaud, A., Xu, Z. J. (2019). Mastering surface reconstruction of metastable spinel oxides for better water oxidation. *Advanced materials*, 31(12), 1807898.
- [2] Zaichuk, A. V., Amelina, A. A. (2019) Blue-green spinel-type ceramic pigments prepared from the slag of aluminothermal production of ferrotitanium. *Voprosy Khimii i Khimicheskoi Tekhnologii*, 4, 46–54.
- [3] Zhao, X., Mao, L., Cheng, Q., Li, J. (2020). Two-dimensional Spinel Structured Co-based Materials for High Performance Supercapacitors: A Critical Review. *Chemical Engineering Journal*, 387, 124081.
- [4] Almessiere, M. A., Korkmaz, A., Slimani, Y., Nawaz, M., Ali, S., Baykal, A. (2019). Magneto-optical properties of rare earth metals substituted Co-Zn spinel nanoferrites. *Ceramics International*, 45(3), 3449–3458.
- [5] Silva, F. G. D., Depeyrot, J., Campos, A. F. C., Aquino, R., Fiorani, D., Peddis, D. (2019). Structural and Magnetic Properties of Spinel Ferrite Nanoparticles. *Journal of nanoscience and nanotechnology*, 19(8), 4888–4902.
- [6] Slimani, Y., Almessiere, M. A., Sertkol, M., Shirsath, S. E. (2019). Structural, magnetic, optical properties and cation distribution of nanosized Ni_{0.3}Cu_{0.3}Zn_{0.4}Tm_xFe_{2-x}O₄ (0.0 ≤ x ≤ 0.10) spinel ferrites synthesized by ultrasound irradiation. *Ultrasonics sonochemistry*, 57, 203–211.
- [7] Rani, M., Shanker, U. (2018). Efficient photocatalytic degradation of Bisphenol A by metal ferrites

- nanoparticles under sunlight. *Environmental Technology & Innovation*, 100792.
- [8] Lassoued, A., Li, J. F. (2020). Magnetic and photocatalytic properties of Ni-Co ferrites *Solid State Sciences*, 106199.
- [9] Javed, H., Rehman, A., Mussadiq, S., Shahid, M., Warsi, M. F. (2019). Reduced graphene oxide-spinel ferrite nano-hybrids as magnetically separable and recyclable visible light driven photocatalyst. *Synthetic Metals*, 254, 1-9.
- [10] Amulya, M. A. S., Nagaswarupa, H. P., Kumar, M.R.A., Ravikumar, C. R., Prashantha, S. C., Kusuma, K.B. (2020). Sonochemical synthesis of NiFe₂O₄ nanoparticles: Characterization and their photocatalytic and electrochemical applications. *Applied Surface Science Advances*, 1, 100023.
- [11] Fadillah, G., Saleh, T. A., Wahyuningsih, S. (2019). Enhanced electrochemical degradation of 4-Nitrophenol molecules using novel Ti/TiO₂-NiO electrodes. *Journal of Molecular Liquids*, 289, 111108.
- [12] Sokolsky, G. V., Zahornyi, M. N., Lobunets, T. F., Tyschenko, N. I., Shyrovkov, A. V., Ragulya, A. V., Zudina, L. V. (2019). Photoelectrocatalytic degradation of amino-azodyes by titanium dioxide with surface states of Ti³⁺. *Journal of Chemistry and Technologies*, 27(2), 130-140.
- [13] Ayodhya, D., Veerabhadram, G. (2019). Influence of g-C₃N₄ and g-C₃N₄ nanosheets supported CuS coupled system with effect of pH on the catalytic activity of 4-NP reduction using NaBH₄. *Chemistry of Flat Materials*, 14, 100088.
- [14] Abdullah, H., Kuo, D. H. (2019). Utilization of photocatalytic hydrogen evolved (Zn, Sn)(O, S) nanoparticles to reduce 4-nitrophenol to 4-aminophenol. *International Journal of Hydrogen Energy*, 44(1), 191-201.
- [15] Liao, G., Gong, Y., Zhong, L., Fang, J., Zhang, L., Xu, Z., Fang, B. (2019). Unlocking the door to highly efficient Ag-based nanoparticles catalysts for NaBH₄-assisted nitrophenol reduction. *NanoResearch*, 1-30.
- [16] Kharisov, B. I., Dias, H. R., Kharissova, O. V. (2019). Mini-review: ferrite nanoparticles in the catalysis. *Arabian Journal of Chemistry*, 12(7), 1234-1246.
- [17] Frolova, L. (2020). Photocatalytic activity of spinel ferrites Co_xFe_{3-x}O₄ (0.25 < x < 1) obtained by treatment contact low-temperature non-equilibrium plasma. *Applied Nanoscience*, 1-6.
- [18] Dey, C., De, D., Nandi, M., Goswami, M. M. (2020). A high performance recyclable magnetic CuFe₂O₄ nanocatalyst for facile reduction of 4-nitrophenol. *Materials Chemistry and Physics*, 242, 122237.
- [19] Almessiere, M. A., Slimani, Y., Sertkol, M., Khan, F. A., Nawaz, M., Tombuloglu, H., Baykal, A. (2019). Ce-Nd Co-substituted nanospinel cobalt ferrites: an investigation of their structural, magnetic, optical, and apoptotic properties. *Ceramics International*, 45(13), 16147-16156.
- [20] Anke, S., Falk, T., Bendt, G., Sinev, I., Hävecker, M., Antoni, H., Cuenya, B. R. (2020). On the reversible deactivation of cobalt ferrite spinel nanoparticles applied in selective 2-propanol oxidation. *Journal of Catalysis*, 382, 57-68.
- [21] Padervand, M., Vossoughi, M., Yousefi, H., Salari, H., Gholami, M. R. (2014). An experimental and theoretical study on the structure and photoactivity of XFe₂O₄ (X= Mn, Fe, Ni, Co, and Zn) structures. *Russian Journal of Physical Chemistry A*, 88(13), 2451-2461.
- [22] Anupama, A. V., Kumaran, V., Sahoo, B. (2019). Synthesis of highly magnetic Mn-Zn ferrite (Mn_{0.7}Zn_{0.3}Fe₂O₄) ceramic powder and its use in smart magnetorheological fluid. *Rheologica Acta*, 58(5), 273-280.
- [23] Melo, R. S., Banerjee, P., Franco, A. (2018). Hydrothermal synthesis of nickel doped cobalt ferrite nanoparticles: optical and magnetic properties. *Journal of Materials Science: Materials in Electronics*, 29(17), 14657-14667.
- [24] Yazdi, S. T., Iranmanesh, P., Saeednia, S., & Mehran, M. (2019). Structural, optical and magnetic properties of Mn_xFe_{3-x}O₄ nanoferrites synthesized by a simple capping agent-free coprecipitation route. *Materials Science and Engineering: B*, 245, 55-62.
- [25] Frolova, L., Pivovarov, A., Butyrina, T. (2017). Synthesis of pigments in Fe₂O₃-Al₂O₃-CoO by co-precipitation method. *Pigment & Resin Technology*, 46(5), 356-361. <https://doi.org/10.1108/PRT-07-2016-0073>
- [26] Frolova, L., Pivovarov, A., Tsepich, E. (2016). Non-equilibrium plasma-assisted hydrophase ferritization in Fe²⁺-Ni²⁺-SO₄²⁻-OH⁻ System. *Nanophysics, Nanophotonics, Surface Studies, and Applications. Springer Proceedings in Physics*, 183, 213-220.
- [27] Frolova, L., Pivovarov, A., Tsepich, E. (2016). Ultrasound ferritization in Fe²⁺-Ni²⁺-SO₄²⁻-OH⁻ system. *Journal of Chemical Technology and Metallurgy*, 51(2), 163-167.
- [28] Frolova, L. A., Derhachov, M. P. (2017). The Effect of Contact Non-equilibrium Plasma on Structural and Magnetic Properties of Mn_xFe_{3-x}O₄ Spinel. *Nanoscale research letters*, 12(1), 505.
- [29] Frolova, L., Derimova, A., Butyrina, T. (2018). Structural and magnetic properties of cobalt ferrite nanopowders synthesis using contact non-equilibrium plasma. *Acta Physica Polonica A*, 133(4), 1021-1023.